Railton, C. J. (1993). An algorithm for the treatment of curved metallic laminas in the finite difference time domain method. IEEE Transactions on Microwave Theory and Techniques, 41(8), 1429 - 1438. 10.1109/22.241685

An Algorithm for the Treatment of Curved Metallic Laminas in the Finite Difference Time Domain Method

C. J. Railton

Abstract—**The Finite Difference Time Domain (FDTD) method, implemented in Cartesian coordinates, is well proven as an efficient technique for the electromagnetic analysis of a wide variety of microwave structures. The standard FDTD method is, however, less efficient if the structure under investigation has boundaries which are not parallel to the coordinate axes. Techniques designed to overcome this problem such as locally or globally deformed grids, or the use of nonorthogonal coordinate systems have been reported but these impose a penalty in computational effort or in flexibility. In this contribution, an alternative technique is described whereby the standard Cartesian grid is maintained, and the existence of the material boundaries is accounted for by the use of special finite difference equations for the affected nodes. These equations take account not only of the position of the boundaries but also of the asymptotic field behavior in their vicinity. This technique results in a flexible, accurate, and efficient, implementation which is applicable to a wide range of MMIC and antenna structures.**

I. Introduction

MANY STRUCTURES such as printed antennas [1], circuit elements [2], [3], and scatterers for which electromagnetic analysis is desired contain metal boundaries which can not all be made parallel to a set of Cartesian or other orthogonal coordinate axes. Whereas the standard Finite Difference time Domain (FDTD) technique is well proven as an efficient method of analyzing structures whose boundaries are all parallel to the coordinate axes, the accuracy and efficiency deteriorates if the structure under investigation contains boundaries at arbitrary angles. Several methods have been proposed in the literature to overcome this problem, the simplest being to resort to the use of a very fine mesh [2]. This approach, however, is likely to yield a computationally inefficient solution to the problem and often leads to a formulation which does not converge to the correct answer no matter how fine a mesh is used [4]. More sophisticated solutions include the use of "deformed" grids in the neighborhood of the material boundary. Here the Cartesian mesh is retained over the majority of the problem space but, in the vicinity of material boundaries, it is made to conform to them. This approach has been successfully used in [5] for the analysis of scattering from a smooth surface. As an alternative, several researchers have investigated the use of conformal grids which use nonorthogonal coordinate systems [6]–[9]. While good results have been obtained using this method, the computation time is stated to be much longer (of the order of 3 times) than the equivalent algorithm using Cartesian coordinates. In addition there is the associated problem of generating a suitable nonorthogonal mesh which is, in itself, a difficult process. A combination of Cartesian and Cylindrical coordinates has been used for the analysis of coaxial waveguide structures in [10], and this treatment is one of the few in which the singular field behavior is accounted for. In this contribution, a different approach is described in which the Cartesian grid with its inherent efficiency and simplicity is maintained, but in which use is made of special Finite Difference (FD) equations in the vicinity of material boundaries. Special algorithms for electrically small structures have been previously used with success in the cases of slots [11], [12], and wires [13]. The analysis of irregularly shaped planar structures has also been addressed in a two-dimensional formulation [14]. Recently, we have demonstrated the incorporation of static field solutions into the FDTD algorithm, which include the effects of the singularities in the field distribution, in order to analyze isolated edges [15] and narrow microstrip where the edges are closer than or comparable to the mesh size [16]. A major advantage of this scheme over the use of nonorthogonal coordinate systems is that the amount of extra computer time required is very small. Moreover, this small penalty is amply compensated by the ability to reduce the density of the mesh while maintaining accuracy. In addition, the generation of the FD equations is an easily automated process which does not introduce the difficulties associated with the generation of a nonorthogonal mesh. This work is now extended to the use of static solutions for the case of metal laminas with curved boundaries such as are often found in microstrip circuits and antennas. The approach is more flexible than the grid deformation approach and, in addition, the field behavior in the region of edges and corners is automatically included. Thus the unit cell size need to be chosen only by consideration of the wavelengths of interest and not be constrained by the size or position of the laminas. This greatly eases the process of mesh generation and leads to a more computationally efficient formulation. The technique may readily be extended to solid objects and objects with edges, corners, or points.

Manuscript received August 11, 1992; revised January 4, 1993. This work was supported in part by the Science and Engineering Research Council, U.K.

The author is with the Centre for Communications Research, Faculty of Engineering, University of Bristol, Bristol BS8 1TR, England.

IEEE Log Number 9210232.

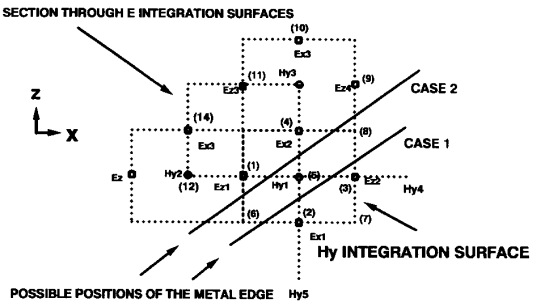

Fig. 1. FDTD grid for calculation of E_x, E_z, and H_y.

II. Definition of the Material Boundary

In Fig. 1, we see the edge of a curved metal lamina lying in the x–z plane which cuts the FDTD mesh. Following standard practice, in order to calculate the new value of the H_y nodes we need the surface integral of H_y and the line integrals of E_z and E_x. If we approximate the edge cutting the mesh by a straight line which makes an angle θ with the x axis we can make use of the known assymptotic forms of the field components tangential and normal to the edge, in order to evaluate the integrals. Thus, we may calculate the coefficients of the FDTD equations which will be functions of both the position of the edge and the angle of the target to the edge.

We define a curved planar lumina by the following functions:

1) *Normaldist* (x, z)*:* returns length of the normal from the point (x, z) to the edge of the lamina projected into the plane of the metal.

2) *Tangentdist* (x, z)*:* returns distance along the edge of the intersection of the normal from the point (x, z) with the lamina with respect to a suitable origin.

3) *Tangentangle* (x)*:* returns the angle of the tangent to the lamina at point x.

4) *Inside* (x, y, z)*:* true if the point (x, y, z) lies on the lamina or false otherwise.

As an example, consider a disk of infinitesimal thickness whose centre is at coordinates (x_0, y_0, z_0) and of radius a. The functions for this case are given by (1).

$$\begin{aligned}\text{Normaldist}\,(x,z) &= \sqrt{(x-x_0)^2+(z-z_0)^2}-a\\ \text{Tangentangle} &= \pm\text{Sin}^{-1}\left(\frac{x-x_0}{a}\right)\\ \text{Inside} &= ((x-x_0)^2+(z-z_0)^2<a^2)\wedge(y=y_0).\end{aligned} \tag{1}$$

III. The Calculation of $\partial H_y/\partial t$ in the Plane of the Metal

Depending on the relative position of the edge of the lamina and the grid, a number of different cases must be identified and dealt with. We consider all H_y nodes whose associated surface of integration intersects the metal lamina as requiring special treatment. Two different cases within this category are then identified, depending on whether the H_y node is on the metal or not. These cases are shown in Fig. 1. In the latter case, the only action which need be taken is to set the H_y node to zero. For the former case and referring to Fig. 1, we see that there can never be less than two (or more than four) E field nodes outside the metal. From the magnitude of the E field at these nodes we estimate the magnitudes of the components of the E field normal and tangential to the metal edge.

Denoting the component of the E field tangential to the edge as E_T and the component normal to the edge and in the plane of the metal as E_N, we expand the field function as follows:

$$E_T(n) = k_1 n P_{ET}(n) + k_2 P_{ET}(n) \tag{2}$$

$$E_N(n,t) = k_3 t P_{EN}(n) + k_4 P_{EN}(n) \tag{3}$$

where n is the length of the normal to the edge of the metal defined by the function Normaldist (x, z) and t is the tangential distance along the edge referred to a suitable origin. It is noted that the values of n and t are independent of the value of y. The functions P_{EN} and P_{ET} are the static E field functions associated with a metal edge. They are given by consideration of the Green's function for a slab loaded waveguide and the well used approximation to the current distribution across a microstrip line as carried out in [17]. If we consider distances from the edge which are electrically small, which an FDTD cell must be, the field distribution is independent of frequency. Under these conditions, it has been found that the assymptotic form of the field pattern, denoted $\boldsymbol{E}^{\infty}$ in [17], is a good approximation to the actual field distribution. Since, at this stage, we are concerned only with the fields in the plane of the metal, we set y to zero.

$$P_{EN} = \text{Im}\left(\frac{\sqrt{2u}}{\sqrt{u^2+(j(n+u)+y)^2}}\right) \tag{4}$$

$$P_{ET} = \text{Re}\left(\sqrt{\frac{u}{2}}\,\text{Log}\left(\frac{u}{y+j(n+u)+\sqrt{u^2+(j(n+u)+y)^2}}\right)\right) \tag{5}$$

where, if the edge is a part of a strip, the parameter u is its half width. For other cases, such as a large or irregularly shaped patch where a width is not simply defined, we let u approach infinity yielding equations (6) and (7) which express the well-known asymptotic field behavior near a single edge.

$$P^{\infty}_{EN} = \text{Im}\left(\frac{1}{\sqrt{jy-n}}\right) \tag{6}$$

$$P^{\infty}_{ET} = \text{Re}\sqrt{n-jy}\,. \tag{7}$$

The Cartesian components of the fields are then expressed as

$$E_x = E_T\,\text{Cos}\,\theta - E_N\,\text{Sin}\,\theta \tag{8}$$

$$E_z = E_T\,\text{Sin}\,\theta + E_N\,\text{Cos}\,\theta \tag{9}$$

We can then express the magnitudes of the fields at each node on the integration surface in terms of the normal and tangential components as follows:

$$\begin{aligned}E_{x1} = {} & k_1 n_2 P_{ET}(n_2)\,\text{Cos}\,\theta + k_2 P_{ET}(n_2)\,\text{Cos}\,\theta\\ & - k_3 t_2 P_{EN}(n_2)\,\text{Sin}\,\theta - k_4 P_{EN}(n_2)\,\text{Sin}\,\theta\end{aligned} \tag{10}$$

$$E_{x2} = k_1 n_4 P_{ET}(n_4)\,\mathrm{Cos}\,\theta + k_2 P_{ET}(n_4)\,\mathrm{Cos}\,\theta - k_3 t_4 P_{EN}(n_4)\,\mathrm{Sin}\,\theta - k_4 P_{EN}(n_4)\,\mathrm{Sin}\,\theta \quad (11)$$

$$E_{z1} = k_1 n_1 P_{ET}(n_1)\,\mathrm{Sin}\,\theta + k_2 P_{ET}(n_1)\,\mathrm{Sin}\,\theta + k_3 t_1 P_{EN}(n_1)\,\mathrm{Cos}\,\theta + k_4 P_{EN}(n_1)\,\mathrm{Cos}\,\theta \quad (12)$$

$$E_{z2} = k_1 n_3 P_{ET}(n_3)\,\mathrm{Sin}\,\theta + k_2 P_{ET}(n_3)\,\mathrm{Sin}\,\theta + k_3 t_3 P_{EN}(n_3)\,\mathrm{Cos}\,\theta + k_4 P_{EN}(n_3)\,\mathrm{Cos}\,\theta \quad (13)$$

where the subscripts refer to the positions of the nodes and the corners of the integration surface as shown by the numbers in brackets in Fig. 1.

For the nodes which are on the metal, the associated equations degenerate to the trivial case of zero = zero.

Since we have four unknowns and may have as few as two nontrivial equations, we must assume some of the k's to be zero. To maintain congruence with the basic FDTD algorithm we do so as follows: if we have three nodes we set k_1 to zero, if we have two nodes then we set k_1 and k_3 to zero.

Equations (10)–(13) can be expressed in matrix form as follows:

$$\underline{\underline{\boldsymbol{A}}}\,\underline{\boldsymbol{k}} = \underline{\boldsymbol{E}} \quad (14)$$

where the matrix $\boldsymbol{A}$ is given by (15) below. And the vectors $\boldsymbol{k}$ and $\boldsymbol{E}$ are given by$(k_1 k_2 k_3 k_4)^T$ and $(E_{x1}E_{x2}E_{z1}E_{z2})^T$, respectively.

If some of the nodes lie on the metal then the corresponding rows and columns of the matrix are removed. For example, if three nodes on the surface of integration are outside the metal then we have a set of linear equations which relate k_2, k_3, and k_4 to the values of the E field nodes such as those shown in (16).

$$\begin{pmatrix} P_{ET}(n_4)\,\mathrm{Cos}\,\theta & -t_4 P_{EN}(n_4)\,\mathrm{Sin}\,\theta & -P_{EN}(n_4)\,\mathrm{Sin}\,\theta \\ P_{ET}(n_1)\,\mathrm{Sin}\,\theta & t_1 P_{EN}(n_1)\,\mathrm{Cos}\,\theta & P_{EN}(n_1)\,\mathrm{Cos}\,\theta \\ P_{ET}(n_3)\,\mathrm{Sin}\,\theta & t_3 P_{EN}(n_3)\,\mathrm{Cos}\,\theta & P_{EN}(n_3)\,\mathrm{Cos}\,\theta \end{pmatrix} \cdot \begin{pmatrix} k_2 \\ k_3 \\ k_4 \end{pmatrix} = \begin{pmatrix} E_{x2} \\ E_{z1} \\ E_{z2} \end{pmatrix}. \quad (16)$$

The line and surface integrals which we need in order to get the coefficients for the FDTD equation as shown in (17) to (19).

$$\int E_x\,d_x = k_1 \mathrm{Cos}\,\theta \int n P_{ET}(n)\,dx + k_2 \mathrm{Cos}\,\theta \int P_{ET}(n)\,dx - k_3\,\mathrm{Sin}\,\theta \int t P_{EN}(n)\,dx - k_4\,\mathrm{Sin}\,\theta \int P_{EN}(n)\,dx \quad (17)$$

$$\int E_z\,dz = k_1 \mathrm{Sin}\,\theta \int n P_{ET}(n)\,dz + k_2\,\mathrm{Sin}\,\theta \int P_{ET}(n)\,dz + k_3\,\mathrm{Cos}\,\theta \int t P_{EN}(n)\,dz + k_4\,\mathrm{Cos}\,\theta \int P_{EN}(n)\,dz \quad (18)$$

$$\iint H_y\,dx\,dz = \frac{H_{y1} \iint P_{HY}(n)\,dx\,dz}{P_{HY}(n_5)} \quad (19)$$

where the function $P_{HY}(n)$ is the asymptotic behavior of the H_y field given by

$$P_{HY} = \mathrm{Im}\left(\frac{\sqrt{2u}}{\sqrt{u^2 + (j(n+u)+y)^2}} \right). \quad (20)$$

Making use of (17)–(19) the integral form of the FDTD equation can be expressed as (21) or in matrix form as (22) where the vector $\boldsymbol{b}$ is made up of the coefficients of $\boldsymbol{k}$ in (21)

$$\begin{aligned} &\frac{\partial \boldsymbol{H}_{y1}}{\partial t} \frac{1}{P_{HY}(n_5)} \int_{z1}^{z2}\int_{x1}^{x2} \mu P_{HY}(n)\,dx\,dz \\ &= k_2\,\mathrm{Cos}\,\theta \left(\int_{x1}^{x2} P_{ET}(x,y,z_1)\,dx - \int_{x1}^{x2} P_{ET}(x,y,z_2)\,dx \right) \\ &\quad + k_1\,\mathrm{Cos}\,\theta \left(\int_{x1}^{x2} n(x,y,z_1) P_{ET}(x,y,z_1)\,dx - \int_{x1}^{x2} n(x,y,z_2) P_{ET}(x,y,z_2)\,dx \right) \\ &\quad - k_4\,\mathrm{Sin}\,\theta \left(\int_{x1}^{x1} P_{EN}(x,y,z_1)\,dx - \int_{x1}^{x2} P_{EN}(x,y,z_2)\,dx \right) \\ &\quad - k_3\,\mathrm{Sin}\,\theta \left(\int_{x1}^{x2} t(x,y,z_1) P_{EN}(x,y,z_1)\,dx - \int_{x1}^{x2} t(x,y,z_2) P_{EN}(x,y,z_2)\,dx \right) \\ &\quad - k_2\,\mathrm{Sin}\,\theta \left(\int_{z1}^{z2} P_{ET}(x_1,y,z)\,dz - \int_{z1}^{z2} P_{ET}(x_2,y,z)\,dz \right) \end{aligned}$$

$$\begin{pmatrix} n_2 P_{ET}(n_2)\,\mathrm{Cos}\,\theta & P_{ET}(n_2)\,\mathrm{Cos}\,\theta & -t_2 P_{EN}(n_2)\,\mathrm{Sin}\,\theta & -P_{EN}(n_2)\,\mathrm{Sin}\,\theta \\ n_4 P_{ET}(n_4)\,\mathrm{Cos}\,\theta & P_{ET}(n_4)\,\mathrm{Cos}\,\theta & -t_4 P_{EN}(n_4)\,\mathrm{Sin}\,\theta & -P_{EN}(n_4)\,\mathrm{Sin}\,\theta \\ n_1 P_{ET}(n_1)\,\mathrm{Sin}\,\theta & P_{ET}(n_1)\,\mathrm{Sin}\,\theta & t_1 P_{EN}(n_1)\,\mathrm{Cos}\,\theta & P_{EN}(n_1)\,\mathrm{Cos}\,\theta \\ n_3 P_{ET}(n_3)\,\mathrm{Sin}\,\theta & P_{ET}(n_3)\,\mathrm{Sin}\,\theta & t_3 P_{EN}(n_3)\,\mathrm{Cos}\,\theta & P_{EN}(n_3)\,\mathrm{Cos}\,\theta \end{pmatrix} \quad (15)$$

$$- k_1 \operatorname{Sin}\theta\left(\int_{z1}^{z2} n(x_1,y,z)P_{ET}(x_1,y,z)\,dz - \int_{z1}^{z2} n(x_2,y,z)P_{ET}(x_2,y,z)\,dz\right)$$
$$- k_4 \operatorname{Cos}\theta\left(\int_{z1}^{z2} P_{EN}(x_1,y,z)\,dz - \int_{z1}^{z2} P_{EN}(x_2,y,z)\,dz\right)$$
$$- k_3 \operatorname{Cos}\theta\left(\int_{z1}^{z2} t(x_1,y,z)P_{EN}(x_1,y,z)\,dz - \int_{z1}^{z2} t(x_2,y,z)P_{EN}(x_2,y,z)\,dz\right) \quad (21)$$

$$\underline{\boldsymbol{b}}\,\underline{\boldsymbol{k}} = \frac{\partial \boldsymbol{H}_{y1}}{\partial t} \quad (22)$$

Combining (14) and (22), we get the required equation for updating the H_{y1} node value:

$$\frac{\partial \boldsymbol{H}_{y1}}{\partial t} = \left(\underline{\boldsymbol{A}}^{-1}\right)^T \underline{\boldsymbol{b}}\,\underline{\boldsymbol{E}}. \quad (23)$$

In general, the matrix $\boldsymbol{A}$ and the vector $\boldsymbol{b}$ are of order n where n is the number of E field nodes on the surface of integration and which are not on the metal surface. The elements of the matrix $(\boldsymbol{A}^{-1})^T\boldsymbol{b}$ are calculated during the setting up stage so that the time required by the main iteration algorithm is not increased.

It is noted that, in the absence of a metal edge, the matrix reduces to (24) which corresponds to the standard FDTD equation

$$\left(\frac{1}{\delta x} - \frac{1}{\delta x}\frac{1}{\delta z} - \frac{1}{\delta z}\right). \quad (24)$$

In Figs. 2, 3, and 4 examples are shown of the coefficients of the special FDTD equations for a situation similar to that shown in Fig. 1 for the case of an edge making an angle θ to the x axis and which passes through the point (0.5 α). The mesh size is set to unity in each direction. The situation for $\theta = 0$, is equivalent to the case treated in [15] and the coefficients for the nonzero nodes are equal to the "correction factors" used there. It can be seen that the coefficients are different when the edge is sloping. The discontinuities which appear in Fig. 2 and Fig. 3 occur at the point where the edge intersects the E_{z2} node.

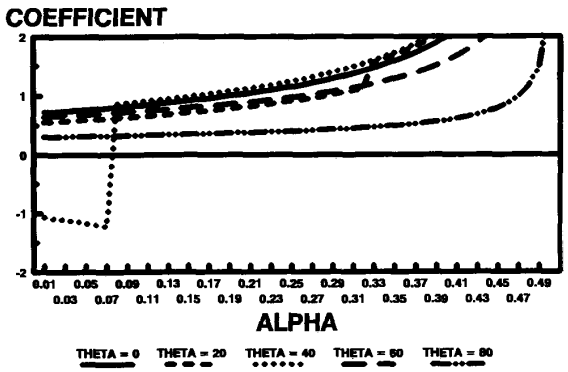

Fig. 2. Calculation of $\partial H_y/\partial t$ - coefficient for the E_x node.

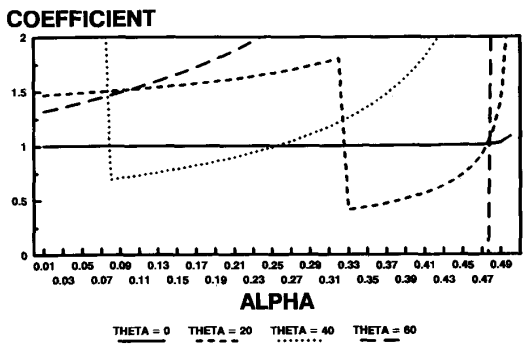

Fig. 3. Calculation of $\partial H_y/\partial t$ - coefficient for the E_{z1} node.

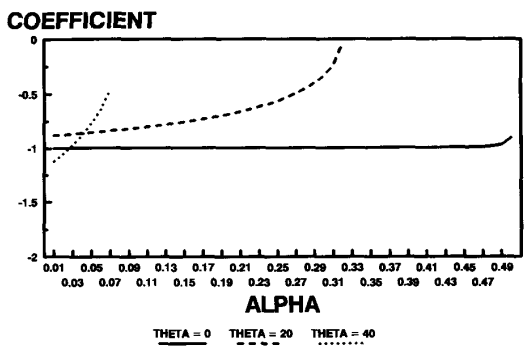

Fig. 4. Calculation of $\partial H_y/\partial t$ - coefficient for the E_{z2} node.

IV. The Calculation of $\partial \boldsymbol{E}_x/\partial t$ and $\partial \boldsymbol{E}_z/\partial t$—Case 1, $\boldsymbol{H}_{y1}$ Outside the Metal

When the metal edge is not parallel to the coordinate axes, the FDTD equations for E_x and E_z are not independent and must be taken together. A way of doing this is to consider a cross which is centered on the H_y node as shown in Fig. 1. In this case, we wish to use special FD equations for whichever of the nodes $E_{x1}E_{x2}E_{z1}$ and E_{z2} are not inside the metal. We make use of (14) in order to relate the values of the vector $\boldsymbol{k}$ for the surface under consideration to the nodes $E_{x1}E_{x2}E_{z1}$ and E_{z2} nodes which are outside the metal region. We also require extra parameters $h_1 - h_8$ which are defined in terms of the H field in the planes above and below the plane of the metal. First, we make the following definitions:

$$P_{HN} = \operatorname{Re}\left(\frac{\sqrt{2u}}{\sqrt{u^2 + (j(n+u)+y)^2}}\right) \quad (25)$$

$$P_{HT} = \operatorname{Im}\left(\sqrt{\frac{u}{2}}\operatorname{Log}\left(\frac{u}{y + j(n+u) + \sqrt{u^2 + (j(n+u)+y)^2}}\right)\right) \quad (26)$$

$$P_{EY} = \mathrm{Re}\left(\frac{\sqrt{2u}}{\sqrt{u^2 + (j(n+u)+y)^2}}\right) \tag{27}$$

where P_{HN} is proportional to the component of the H field normal to the edge and P_{HT} is proportional to the component tangential to the edge. We then expand the H field components normal and tangential to the edge and in the plane half a unit cell above the plane of the metal as:

$$H_T(n) = h_1 n P_{HT}(n) + h_2 P_{HT}(n) \tag{28}$$

$$H_N(n,t) = h_3 t P_{HN}(n) + h_4 P_{HN}(n)\,. \tag{29}$$

The Cartesian components of the H field above and below the plane of metallization are then expressed as:

$$H_x(y_1) = h_1 n(y_1) P_{HT}\,\mathrm{Cos}\,\theta + h_2 P_{HT}(y_1)\,\mathrm{Cos}\,\theta - h_3 t P_{HN}(y_1)\,\mathrm{Sin}\,\theta - h_4 P_{HN}(y_1)\,\mathrm{Sin}\,\theta \tag{30}$$

$$H_z(y_1) = h_1 n P_{HT}(y_1)\,\mathrm{Sin}\,\theta + h_2 P_{HT}(y_1)\,\mathrm{Sin}\,\theta + h_3 t P_{HN}(y_1)\,\mathrm{Cos}\,\theta + h_4 P_{HN}(y_1)\,\mathrm{Cos}\,\theta \tag{31}$$

$$H_x(y_{-1}) = h_5 n(y_{-1}) P_{HT}\,\mathrm{Cos}\,\theta + h_6 P_{HT}(y_{-1})\,\mathrm{Cos}\,\theta - h_7 t P_{HN}(y_{-1})\,\mathrm{Sin}\,\theta - h_8 P_{HN}(y_{-1})\,\mathrm{Sin}\,\theta \tag{32}$$

$$H_z(y_{-1}) = h_5 n P_{HT}(y_{-1})\,\mathrm{Sin}\,\theta + h_6 P_{HT}(y_{-1})\,\mathrm{Sin}\,\theta + h_7 t P_{HN}(y_{-1})\,\mathrm{Cos}\,\theta + h_8 P_{HN}(y_{-1})\,\mathrm{Cos}\,\theta \tag{33}$$

where the plane $y = y_1$ is half a unit cell above the plane of the metallization.

Using (30)–(33), we can express the values of the H field nodes as follows:

$$\underline{\boldsymbol{H}} = \underline{\underline{\boldsymbol{F}}}\,\underline{\boldsymbol{h}} \tag{34}$$

where $\boldsymbol{H} = (H_{x1}(y_1)H_{x2}(y_1)H_{z1}(y_1)H_{z2}(y_1)H_{x1}(y_{-1})H_{x2}(y_{-1})H_{z1}(y_{-1})H_{z2}(y_{-1}))^T$, $\boldsymbol{h}$ is the vector made up of $h_1 - h_8$ and the matrix $\boldsymbol{F}$ are the coefficients of $\boldsymbol{h}$ taken from equations (30) to (33). The nodes H_{x1}, etc., are directly above and below the nodes E_{z1} etc.

We now require the integrals given by (35) to (38) from which we can express the FDTD equations for E_z and E_x nodes

$$\iint E_x\,dy\,dz = k_1\,\mathrm{Cos}\,\theta \iint nP_{ET}\,dy\,dz + k_2\,\mathrm{Cos}\,\theta \iint P_{ET}\,dy\,dz - k_3\,\mathrm{Sin}\,\theta \cdot \iint tP_{EN}\,dy\,dz - k_4\,\mathrm{Sin}\,\theta \iint P_{EN}\,dy\,dz \tag{35}$$

$$\iint E_z\,dy\,dz = k_1\,\mathrm{Sin}\,\theta \iint nP_{ET}\,dy\,dz + k_2\,\mathrm{Sin}\,\theta \iint P_{ET}\,dy\,dz + k_3\,\mathrm{Cos}\,\theta \cdot \iint tP_{EN}n\,dy\,dz + k_4\,\mathrm{Cos}\,\theta \iint P_{EN}\,dy\,dz \tag{36}$$

$$\int H_x\,dx = h_1\,\mathrm{Cos}\,\theta \int nP_{HT}\,dx + h_2\,\mathrm{Cos}\,\theta \int P_{HT}\,dx - h_3\,\mathrm{Sin}\,\theta \int tP_{HN}\,dx - h_4\,\mathrm{Sin}\,\theta \int P_{HN}\,dx \tag{37}$$

$$\int H_z\,dz = h_1\,\mathrm{Sin}\,\theta \int nP_{HT}\,dz + h_2\,\mathrm{Sin}\,\theta \int P_{HT}\,dz + h_3\,\mathrm{Cos}\,\theta \int tP_{HN}\,dz + h_4\,\mathrm{Cos}\,\theta \int P_{HN}\,dz\,. \tag{38}$$

The FDTD equations for $\partial E_{x2}/\partial t$ and $\partial E_{z1}/\partial t$ are given by (39) and (40). Similar equations may be written down for the other two nodes

$$\begin{aligned}
&\mathrm{Cos}\,\theta \frac{\partial k_1}{\partial t} \int_{z5}^{z11}\int_{y-1}^{y1} \epsilon(y,z) nP_{ET}\,dy\,dz \\
&\quad + \mathrm{Cos}\,\theta \frac{\partial k_2}{\partial t} \int_{z5}^{z11}\int_{y-1}^{y1} \cdot \epsilon(y,z) P_{ET}\,dy\,dz \\
&\quad - \mathrm{Sin}\,\theta \frac{\partial k_3}{\partial t} \int_{z5}^{z11}\int_{y-1}^{y1} \epsilon(y,z) tP_{EN}\,dy\,dz \\
&\quad - \mathrm{Sin}\,\theta \frac{\partial k_4}{\partial t} \int_{z5}^{z11}\int_{y-1}^{y1} \cdot \epsilon(y,z) P_{EN}\,dy\,dz \\
&= -H_{y3}\delta y + \frac{H_{y1}}{P_{HY}(n_5)} \int_{y-1}^{y1} P_{HY}\,dy \\
&\quad + \mathrm{Sin}\,\theta \left(h_1 \int_{z5}^{z11} nP_{HT}(x,y_1,z)\,dz - h_5 \int_{z5}^{z11} nP_{HT}(x,y_{-1},z)\,dz \right) \\
&\quad + \mathrm{Cos}\,\theta \left(h_3 \int_{z5}^{z11} t(x,y_1,z) P_{HN}(x,y_1,z)\,dz - h_7 \int_{z5}^{z11} t(x,y_{-1},z) P_{HN}(x,y_{-1},z)\,dz \right) \\
&\quad + \mathrm{Sin}\,\theta \left(h_2 \int_{z5}^{z11} dz\, P_{HT}(x,y_1,z) - h_6 \int_{z5}^{z11} dz\, P_{HT}(x,y_{-1},z) \right)
\end{aligned}$$

$$+ \text{Co s}\theta\left(h_4 \int_{z5}^{z11} P_{HN}(x, y_1, z)\, dz - h_8 \int_{z5}^{z11} P_{HN}(x, y_{-1}, z)\, dz \right) \quad (39)$$

$$\begin{aligned}
&\text{Sin } \theta \frac{\partial k_1}{\partial t} \int_{x12}^{x5}\int_{y-1}^{y1} \epsilon(x,y) n P_{ET}\, dy\, dx \\
&\quad + \text{Sin } \theta \frac{\partial k_2}{\partial t} \int_{x12}^{x5}\int_{y-1}^{y1} \epsilon(x,y) P_{ET}\, dy\, dx \\
&\quad + \text{Cos } \theta \frac{\partial k_3}{\partial t} \int_{x12}^{x5}\int_{y-1}^{y1} \epsilon(x,y) t P_{EN}\, dy\, dx \\
&\quad + \text{Cos } \theta \frac{\partial k_4}{\partial t} \int_{x12}^{x5}\int_{y-1}^{y1} \epsilon(x,y) P_{EN}\, dy\, dx \\
&\quad = H_{y2}\delta y - \frac{H_{y1}}{P_{HY}(n_5)} \int_{y-1}^{y1} P_{HY}\, dy \\
&\quad + \text{Cos } \theta \left(h_1 \int_{x12}^{x5} n P_{HT}(x, y_1, z)\, dx - h_5 \int_{x12}^{x5} n P_{HT}(x, y_{-1}, z)\, dx \right) \\
&\quad - \text{Sin } \theta \left(h_3 \int_{x12}^{x5} t(x, y_1, z) P_{HN}(x, y_1, z)\, dx - h_7 \int_{x12}^{x5} t(x, y_{-1}, z) P_{HN}(x, y_{-1}, z)\, dx \right) \\
&\quad + \text{Cos } \theta \left(h_2 \int_{x12}^{x5} dx\, P_{HT}(x, y_1, z) - h_6 \int_{x12}^{x5} dx\, P_{HT}(x, y_{-1}, z) \right) \\
&\quad - \text{Sin } \theta \left(h_4 \int_{x12}^{x5} P_{HN}(x, y_1, z)\, dx - h_8 \int_{x12}^{x5} P_{HN}(x, y_{-1}, z)\, dx \right). \quad (40)
\end{aligned}$$

We may express these equations in matrix form as follows:

$$\underline{\underline{C}} \frac{\partial \underline{k}}{\partial t} = \underline{\underline{D}}\, \underline{H}_y + \underline{\underline{G}}\, \underline{h} \quad (41)$$

where the matrix $\boldsymbol{C}$ is made up of the coefficients of $\partial \boldsymbol{k}/\partial t$, the matrix $\boldsymbol{D}$ are the coefficients of the H_y nodes, the matrix G are the coefficients of $\boldsymbol{h}$ in (39), etc. In general, matrix $\boldsymbol{C}$ is of order $(n \times n)$, matrix $\boldsymbol{D}$ is of order $(n \times n) + 1)$ and matrix $\boldsymbol{G}$ is of order $(n \times 8)$ where n is the number of E field nodes outside the metal.

Since the H_y nodes other than H_{y1} are farther from the edge of the metal, we make the usual FDTD approximation that the value of H_y varies linearly over the limits of integration.

Substituting from (14) and (34), we get the desired special FDTD equation for updating the E field nodes in the vector $\boldsymbol{E}$ as follows:

$$\frac{\partial \underline{\underline{E}}}{\partial t} = \underline{\underline{A}}\, \underline{\underline{C}}^{-1} (\underline{\underline{D}}\, \underline{H}_y + \underline{\underline{G}}\, \underline{\underline{F}}^{-1} \underline{H}). \quad (42)$$

V. The Calculations of $\partial E_x/\partial t$ and $\partial E_z/\partial t$—Case 2 H_{y1} on the Metal

The previous section makes the assumption that the H_{y1} node is outside the metal. If this is not the case, and this node is zero, then we need to calculate the E_{x2} and E_{z1} nodes making use of neighboring E nodes rather than the standard FDTD technique of using the surrounding H nodes.

For the calculation of E_{x2}, we consider the surface which contains the E_{x2} node but does not intersect the metal. In other words, the surface containing $E_{x2}E_{x3}E_{z3}$ and E_{z4}. We can write down the following equations:

$$\begin{aligned}
E_{x3} = {} & k_2 P_{ET}(n_{10}) \text{ Cos } \theta - k_3 t_{10} P_{EN}(n_{10}) \text{ Sin } \theta \\
& - k_4 P_{EN}(n_{10}) \text{ Sin } \theta \quad (43)
\end{aligned}$$

$$\begin{aligned}
E_{x2} = {} & k_2 P_{ET}(n_4) \text{ Cos } \theta - k_3 t_4 P_{EN}(n_4) \text{ Sin } \theta \\
& - k_4 P_{EN}(n_4) \text{ Sin } \theta \quad (44)
\end{aligned}$$

$$\begin{aligned}
E_{z3} = {} & k_{11} P_{ET}(n_1) \text{ Sin } \theta + k_3 t_{11} P_{EN}(n_{11}) \text{ Cos } \theta \\
& + k_4 P_{EN}(n_{11}) \text{ Cos } \theta \quad (45)
\end{aligned}$$

$$\begin{aligned}
E_{z4} = {} & k_2 P_{ET}(n_9) \text{ Sin } \theta + k_3 t_9 P_{EN}(n_9) \text{ Cos } \theta \\
& + k_4 P_{EN}(n_9) \text{ Cos } \theta. \quad (46)
\end{aligned}$$

We make use of the known values of $E_{x3}E_{z3}$ and E_{z4} in order to calculate the values of $k_2 - k_4$. We then use equation (44) to calculate the value of E_{x2}. A similar procedure is used to calculate the value of E_{z1}. It is noted that, for edges parallel to the axis, this approach reduces to that used successfully in [16].

VI. Calculations of $\partial H_x/\partial t$ and $\partial H_z/\partial t$ Above and Below the Plane of the Metal

Since the nodes H_x and H_z directly above and below the nodes for E_z and E_x makes use of the E nodes close to the edge, they must also be dealt with. This is especially important when large values have been used for the coefficients in equations for the other special FD equations.

Corresponding to (14), we can write equations which express the E field in the planes $y = +/-2$ above and below the plane of metallization as follows:

$$\underline{\underline{A}}_+ \underline{k}_+ = \underline{E}_+ \quad (47)$$

$$\underline{\underline{A}}_- \underline{k}_- = \underline{E}_- \quad (48)$$

where the subscripts + and − indicate the planes one unit cell above and below the plane of metallization, respectively.

In order to update the H nodes above and below the plane of the metal we require the integrals given by (49) to (55)

from which we can express the FDTD equations for $H_{x1}(y1)$ and $H_{z2}(y1)$ as (56) and (57)

$$\iint H_x\,dy\,dz = h_1 \operatorname{Cos}\theta \iint nP_{HT}\,dy\,dz + h_2 \operatorname{Cos}\theta \iint P_{HT}\,dy\,dz - h_3 \operatorname{Sin}\theta \iint tP_{HN}\,dy\,dz - h_4 \operatorname{Sin}\theta \iint P_{HN}\,dy\,dz \tag{49}$$

$$\iint H_z\,dx\,dy = h_1 \operatorname{Sin}\theta \iint nP_{HT}\,dx\,dy + h_2 \operatorname{Sin}\theta \iint P_{HT}\,dx\,dy + h_3 \operatorname{Cos}\theta \iint tP_{HN}n\,dx\,dy + h_4 \operatorname{Cos}\theta \iint P_{HN}\,dx\,dy \tag{50}$$

$$\int E_x(y_2)\,dx = e_1 \operatorname{Cos}\theta \int nP_{ET}\,dx + e_2 \operatorname{Cos}\theta \int P_{ET}\,dx - e_3 \operatorname{Sin}\theta \int tP_{EN}\,dx - e_4 \operatorname{Sin}\theta \int P_{EN}\,dx \tag{51}$$

$$\int E_z(y_2)\,dz = e_1 \operatorname{Sin}\theta \int nP_{ET}\,dz + e_2 \operatorname{Sin}\theta \int P_{ET}\,dz + e_3 \operatorname{Cos}\theta \int tP_{EN}\,dz + e_4 \operatorname{Cos}\theta \int P_{EN}\,dz \tag{52}$$

$$\int E_x(y_{-2})\,dx = e_5 \operatorname{Cos}\theta \int nP_{ET}\,dx + e_6 \operatorname{Cos}\theta \int P_{ET}\,dx - e_7 \operatorname{Sin}\theta \int tP_{EN}\,dx - e_8 \operatorname{Sin}\theta \int P_{EN}\,dx \tag{53}$$

$$\int E_z(y_{-2})\,dz = e_5 \operatorname{Sin}\theta \int nP_{ET}\,dz + e_6 \operatorname{Sin}\theta \int P_{ET}\,dz + e_7 \operatorname{Co}s\theta \int tP_{EN}\,dz + e_8 \operatorname{Cos}\theta \int P_{EN}\,dz \tag{54}$$

$$\int H_y\,dy = \frac{H_{y1}}{P_{HY}(n_5)} \int P_{HY}\,dy \tag{55}$$

$$\begin{aligned}
&\operatorname{Cos}\theta \frac{\partial h_1}{\partial t} \int_{z6}^{z9}\int_{y0}^{y2} \mu nP_{HT}\,dy\,dz + \operatorname{Cos}\theta \frac{\partial h_2}{\partial t} \int_{z6}^{z9}\int_{y0}^{y2} \mu P_{HT}\,dy\,dz - \operatorname{Sin}\theta \frac{\partial h_3}{\partial t} \int_{z6}^{z9}\int_{y0}^{y2} \mu tP_{HN}\,dy\,dz - \operatorname{Sin}\theta \frac{\partial h_4}{\partial t} \int_{z6}^{z9}\int_{y0}^{y2} \mu P_{HN}\,dy\,dz \\
&\quad = \frac{1}{P_{EY}(9)} \int_{y0}^{y2} P_{EY}\,dy - \frac{1}{P_{EY}(6)} \int_{y0}^{y2} P_{EY}\,dy \\
&\quad + \operatorname{Sin}\theta \left(k_1 \int_{z6}^{z9} nP_{ET}(x, y_0, z)\,dz - e_1 \int_{z6}^{z9} nP_{ET}(x, y_2, z)\,dz \right) \\
&\quad + \operatorname{Cos}\theta \left(k_3 \int_{z6}^{z9} t(x, y_0, z) P_{EN}(x, y_0, z)\,dz - e_3 \int_{z6}^{z9} t(x, y_2, z) P_{EN}(x, y_2, z)\,dz \right) \\
&\quad + \operatorname{Sin}\theta \left(k_2 \int_{z6}^{z9} dz P_{ET}(x, y_0, z) - e_2 \int_{z6}^{z9} dz P_{ET}(x, y_2, z) \right) \\
&\quad + \operatorname{Cos}\theta \left(k_4 \int_{z6}^{z9} P_{EN}(x, y_0, z)\,dz - e_4 \int_{z6}^{z9} P_{EN}(x, y_2, z)\,dz \right)
\end{aligned} \tag{56}$$

$$\begin{aligned}
&\operatorname{Sin}\theta \frac{\partial h_1}{\partial t} \int_{x9}^{x8}\int_{y0}^{y2} \mu nP_{HT}\,dy\,dx + \operatorname{Sin}\theta \frac{\partial h_2}{\partial t} \int_{x9}^{x8}\int_{y0}^{y2} \mu P_{HT}\,dy\,dx + \operatorname{Cos}\theta \frac{\partial h_3}{\partial t} \int_{x9}^{x8}\int_{y0}^{y2} \mu tP_{HN}\,dy\,dx + \operatorname{Cos}\theta \frac{\partial h_4}{\partial t} \int_{x9}^{x8}\int_{y0}^{y2} \mu P_{HN}\,dy\,dx \\
&\quad = \frac{1}{P_{EY}(8)} \int_{y0}^{y2} P_{EY}\,dy - \frac{1}{P_{EY}(9)} \int_{y0}^{y2} P_{EY}\,dy \\
&\quad + \operatorname{Cos}\theta \left(k_1 \int_{x9}^{x8} nP_{ET}(x, y_0, z)\,dx \right.
\end{aligned}$$

$$
\begin{aligned}
&- e_1 \int_{x9}^{x8} nP_{ET}(x, y_2, z)\, dx \Bigg) \\
&- \mathrm{Sin}\theta \Bigg(k3 \int_{x9}^{x8} t(x, y_0, z) P_{EN}(x, y_0, z)\, dx \\
&- e_3 \int_{x9}^{x8} t(x, y_2, z) P_{EN}(x, y_2, z)\, dx \Bigg) \\
&\mathrm{Cos}\,\theta \Bigg(k_2 \int_{x9}^{x8} dx P_{ET}(x, y_0, z) \\
&- e_2 \int_{x9}^{x8} dx P_{ET}(x, y_2, z) \Bigg) \\
&- \mathrm{Sin}\,\theta \Bigg(k_4 \int_{x9}^{x8} P_{EN}(x, y_0, z)\, dx \\
&- e_4 \int_{x9}^{x8} P_{EN}(x, y_2, z)\, dx \Bigg).
\end{aligned} \tag{57}
$$

Similar equations may be written for the other six H nodes. We may express these equations in matrix form as follows:

$$
\underline{\underline{K}} \frac{\partial \underline{h}}{\partial t} = \underline{\underline{L}}\, \underline{E_y} + \underline{\underline{M}}\, \underline{e} \tag{58}
$$

where the matrix $\boldsymbol{K}$ is made up of the coefficients of $\partial \boldsymbol{h}/\partial t$, the matrix $\boldsymbol{L}$ is made up of the coefficients of the E_y nodes, the matrix $\boldsymbol{M}$ are the coefficients of $\boldsymbol{e}$ in (56), etc. In general, matrix $\boldsymbol{K}$ is of order (8×8), matrix $\boldsymbol{L}$ is of order (8×10) and matrix $\boldsymbol{M}$ is of order (8×12). The vector $\boldsymbol{e}$ as 12 components and is made up of contribution from the plane of metallization and the planes above and below as follows:

$$
\underline{e} = (e_1\ e_2\ e_3\ e_4\ k_1\ k_2\ k_3\ k_4\ e_5\ e_6\ e_7\ e_8)^T. \tag{59}
$$

Substituting from (14), (34), (47), and (48), we get

$$
\frac{\partial \boldsymbol{H}}{\partial t} = \underline{\underline{F}}\, \underline{\underline{K}}^{-1} (\underline{\underline{L}}\, \underline{E_y} + \underline{\underline{M}}\, \underline{\underline{A_O}}^{-1} \underline{E}) \tag{60}
$$

where the $\boldsymbol{A}_O$ is the 12×12 matrix given by (61) and the vector $\boldsymbol{E}$ is

$$
\begin{aligned}
&(E_{x1}(y_2) E_{x2}(y_2) E_{z1}(y_2) E_{z2}(y_2) E_{x1}(y_0) E_{x2}(y_0) E_{z1}(y_0) \\
&\quad E_{z2}(y_0) E_{x1}(y_{-2}) E_{x2}(y_{-2}) E_{z1}(y_{-2}) E_{z2}(y_{-2}))^T
\end{aligned}
$$

$$
\underline{\underline{A_o}} = \begin{pmatrix} \underline{\underline{A_+}} & \underline{\underline{0}} & \underline{\underline{0}} \\ \underline{\underline{0}} & \underline{\underline{A}} & \underline{\underline{0}} \\ \underline{\underline{0}} & \underline{\underline{0}} & \underline{\underline{A_-}} \end{pmatrix} \tag{61}
$$

VII. Calculation of $\partial E_y/\partial t$ Above and Below the Plane of the Metal

The situation for the calculation of E_y is shown in Fig. 5. Apart from the exchange of roles for the E and H field, the calculation is similar to the procedure used for the calculation of H_y. The main difference is that the metal never cuts the integration surfaces. This means that all four $k's$ and the associated coefficients are always nonzero.

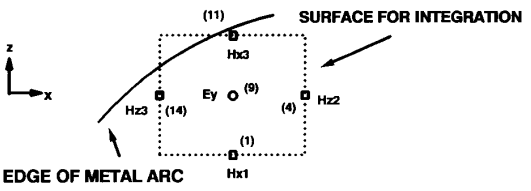

Fig. 5. FDTD grid for calculation of E_y above and below the metal.

Corresponding to equation (14) the values of the H field nodes are expressed as follows:

$$
\underline{\boldsymbol{H}} = \underline{\underline{\boldsymbol{A}_H}}\, \underline{\boldsymbol{k}_H} \tag{62}
$$

where the matrix $\boldsymbol{A}_H$ is given by ? and $\boldsymbol{H} = (H_{x1}(y_1) H_{x3}(y_1) H_{z2}(y_1) H_{z3}(y_1))_T$.

The FDTD equation is then given by (63) or in matrix form by (64).

$$
\begin{aligned}
&\frac{\partial E_y}{\partial t} \frac{1}{P_{EY}(n_{13})} \int_{z1}^{z11} \int_{x14}^{x4} P_{EY}\, dx\, dz = \\
&\quad - k_{H2}\, \mathrm{Sin}\,\theta \Bigg(\int_{x14}^{x4} P_{HN}(x, y, z_1)\, dx \\
&\quad - \int_{x14}^{x4} P_{HN}(x, y, z_{11})\, dx \Bigg) \\
&\quad - k_{H1}\, \mathrm{Sin}\,\theta \Bigg(\int_{x14}^{x4} t(x, y, z_1) P_{HN}(x, y, z_1)\, dx \\
&\quad - \int_{x14}^{x4} t(x, y, z_{11}) P_{HN}(x, y, z_{11})\, dx \Bigg) \\
&\quad + k_{H8}\, \mathrm{Cos}\,\theta \Bigg(\int_{x14}^{x4} dx\, P_{HT}(x, y, z_1) \\
&\quad - \int_{x14}^{x4} dx\, P_{HT}(x, y, z_{11})\, dx \Bigg) \\
&\quad + k_{H7}\, \mathrm{Cos}\,\theta \Bigg(\int_{x14}^{x4} n(x, y, z_1)\, dx P_{HT} n(x, y, z_1) \\
&\quad - \int_{x14}^{x4} n(x, y, z_{11})\, dx P_{HT}(x, y, z_{11}) \Bigg) \\
&\quad - k_{H2}\, \mathrm{Cos}\,\theta \Bigg(\int_{z1}^{z11} P_{Hn}(x_{14}, y, z)\, dz \\
&\quad - \int_{z1}^{z11} P_{HN}(x_4, y, z)\, dz \Bigg) \\
&\quad - k_{H1}\, \mathrm{Cos}\,\theta \Bigg(\int_{z1}^{z11} t(x_{14}, y, z) P_{HN}(x_{14}, y, z)\, dz \\
&\quad - \int_{z1}^{z11} t(x_4, y, z) P_{HN}(x_4, y, z)\, dz \Bigg)
\end{aligned}
$$

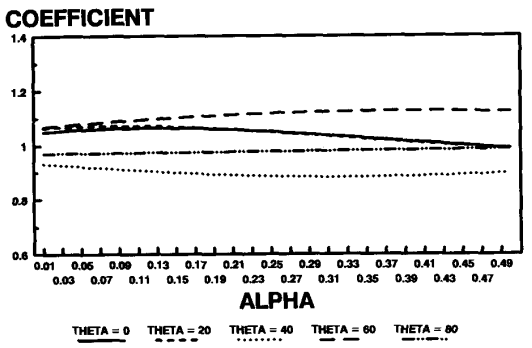

Fig. 6. Calculation of $\partial E_y/\partial t$ - coefficient for the H_{x1} node.

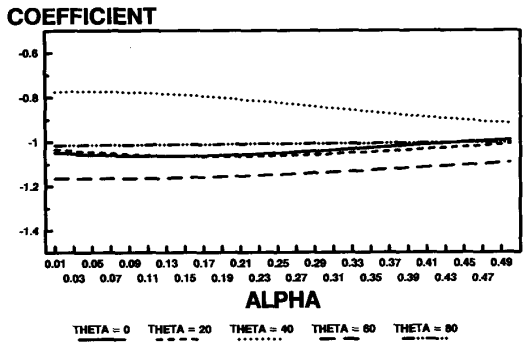

Fig. 7. Calculation of $\partial E_y/\partial t$ - coefficient for the H_{x2} node.

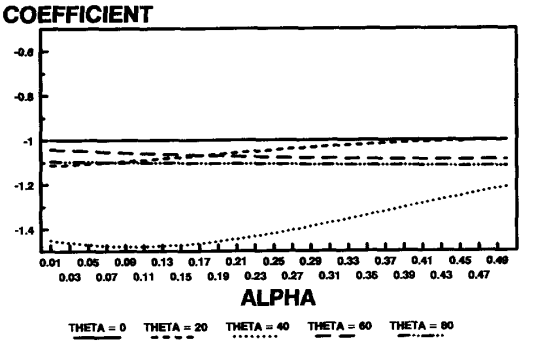

Fig. 8. Calculation of $\partial E_y/\partial t$ - coefficient for the H_{z1} node.

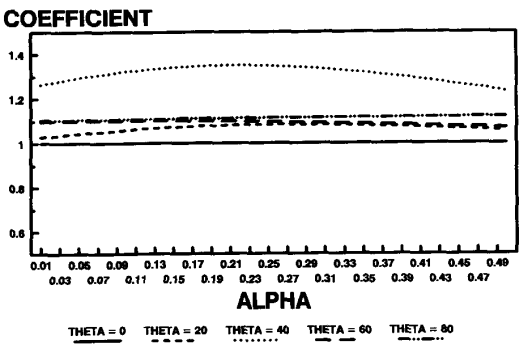

Fig. 9. Calculation of $\partial E_y/\partial t$ - coefficient for the H_{z2} node.

$$- k_{H8} \operatorname{Sin}\theta\left(\int_{z1}^{z11} dz P_{HT}(x_{14}, y, z) - \int_{z1}^{z11} dz P_T(x_4, y, z)\right) - k_{H7} \operatorname{Sin}\theta\left(\int_{z1}^{z11} n(x_{14}, y, z)\, dz P_{HT}(x_{14}, y, z) - \int_{z1}^{z11} n(x_4, y, z)\, dz P_{HT}(x_4, y, z)\right) \tag{63}$$

$$\frac{\partial E_y}{\partial t} = \underline{b_H}\,\underline{k_H}. \tag{64}$$

and the coefficients of the FDTD equation are given by (65)

$$\frac{\partial E_y}{\partial t} = (\underline{\underline{A_H}}^{-1})^T \underline{b_H}\,\underline{H}. \tag{65}$$

Examples of the calculated coefficients for the FDTD equations are shown in Figs. 6–Fig. 9. As before the curves for the case $\theta = 0$, give the values which were used in [15].

VIII. Conclusion

This contribution has described a technique for efficiently analyzing curved metal laminas of the type commonly found in microstrip circuits and antennas, using the FDTD method. In this technique, the efficiency and simplicity of the Cartesian mesh is retained over the whole problem space and special, precomputed, FD equations are used in the vicinity of the metal boundaries. This approach is computationally much more efficient than the staircasing approximation and more computationally efficient than the formulations which make use of nonorthogonal coordinates. In contrast to the local contour deformation method, the asymptotic field solutions are incorporated into the FDTD algorithm which allows the use of a mesh constrained only by the wavelengths of interest. The technique is readily extendable to the cases of solid objects which contain edges, corners or points.

Acknowledgment

The author wishes to thank Professor J. P. McGeehan, Director of the Centre for Communications Research, University of Bristol for the provision of facilities.

References

[1] B. Edward and D. Rees, "A broadband printed dipole with integrated balun," *Microwave Journal*, pp. 389–344, 1987.

[2] S. Maeda, T. Kashiwa, and I. Fukai, "Full wave analysis of propagation characteristics of a through hole using the finite difference time domain method," *IEEE Trans, Microwave Theory Tech.*, vol. MTT-39, pp. 2154–2159, Dec. 1991.

[3] J. Moore and H. Ling "Characterization of a 90° microstrip bend with arbitrary mitre via the time domain finite difference method," *IEEE Trans. Microwave Theory Tech.*, vol. MTT-38, pp. 405–410, Apr. 1990.

[4] A. C. Cangellaris and D. B. Wright, "Analysis of the numerical error caused by the stair-stepped approximation of a conducting boundary

in FDTD simulations of electromagnetic phenomena, *IEEE Trans. Antennas Propagat.* vol. AP-39, pp. 1518–1525, Oct. 1991.
[5] T. G. Jurgens, A. Taflove, K. Umashankar, and T. G. Moore, "Finite-difference time-domain modelling of curved surfaces," *IEEE Trans. Antennas Propagat.* vol. AP-40, no. 4, pp. 357–366, Apr. 1992.
[6] R. Holland "Finite difference solution of Maxwell's equations in generalized nonorthogonal coordinates," *IEEE Trans. Nucl. Sci.,* vol. NS-30, Dec. 1983.
[7] M. Fusco "FDTD algorithm in curvilinear coordinates," *IEEE Trans. Antennas Propagat.* vol. AP-38, pp. 76–88, Jan. 1990.
[8] J. F. Lee, R. Palandech, and R. Mittra "Modelling three-dimensional discontinuities in waveguides using nonorthogonal FDTD algorithm" *IEEE Trans. Microwave Theory Tech.,* vol. MTT-40, pp. 346–352, Feb. 1992.
[9] R. Holland, V. P. Cable, and L. C. Wilson, "Finite volume time domain (FVTD) techniques form EM scattering," *IEEE Trans. Electromagn. Compat.,* vol. EMC-33, pp. 281–294, Nov. 1991.
[10] J. Van Hese and D. De Zutter, "Modelling of discontinuities in general coaxial waveguide structures by the FDTD method," *IEEE Trans. Microwave Theory Tech.,* vol. MTT-40, pp. 547–556, Mar. 1992.
[11] A. Taflove, K. Umashankar, K. Beker, F. Harfoush, and K. Yee, "Detailed FDTD analysis of electromagnetic fields penetrating narrow slots and lapped joints in conducting screens," *IEEE Trans. Antennas Propagat.* vol. AP-36, pp. 247–257, Feb. 1988.
[12] D. J. Riley and C. D. Turner, "The inclusion of wall loss in finite difference time domain thin slot algorithms," *IEEE Trans. Electromagn. Compat.,* vol. EMC-33, pp. 304–311, Nov. 1991.
[13] R. Holland and L. Simpson, "Finite difference analysis of EMP coupling to thin struts and wires," *IEEE Trans. Electromagnet. Compatibil.,* vol. EMC-23, pp. 88–97.
[14] W. K. Gwarek "Analysis of an arbitrarily-shaped planar circuit—A time domain approach," *IEEE Trans. Microwave Theory Tech.,* vol. MTT-33, pp. 1067–1072, Oct. 1985.
[15] D. B. Shorthouse and C. J. Railton, "The incorporation of static field solutions in the finite difference time domain method," *IEEE Trans. Microwave Theory Tech.,* vol. MTT-40, pp. 986–994, May 1992.
[16] C. J. Railton, D. B. Shorthouse, and J. P. McGeehan "The analysis of narrow microstrip lines using the finite difference time domain method." *Electronics Lett.,* pp. 1168–1170, June 1992.
[17] C. J. Railton and J. P. McGeehan, "A rigorous and computationally efficient analysis of microstrip for use as an electro-optic modulator." *IEEE Trans. Microwave Theory Tech.,* vol. MTT-37, pp. 1099–1104, July 1989.

C. J. Railton, (M'88) received the B.Sc. degree (with honors) in physics with electronics from the University of London in 1974 and the Ph.D. degree in electronic engineering from the University of Bath in 1988.

During the period 1974–1984 he worked in the scientific civil service on a number of research and development projects in the areas of communications and signal processing. Between 1984 and 1987 he worked at the University of Bath on the mathematical modelling of boxed microstrip circuits. Dr. Railton currently works in the Centre for Communications Research at the University of Bristol where he leads a group involved in the mathematical modelling and the development of CAD tools for MMICs, antennas, microwave heating systems, EMC and high-speed logic